Bone 78 (2015) 71–80

Contents lists available at ScienceDirect

Bone

journal homepage: www.elsevier.com/locate/bone

Original Full Length Article

Mapping trabecular disconnection "hotspots" in aged human spine and hip

Jean E. Aaron [a,*], Patricia A. Shore [a], Mizuo Itoda [a], Rory J.M. Morrison [a], Andrew Hartopp [a], Elizabeth M.A. Hensor [b], Lesley D. Hordon [a,c]

[a] School of Biomedical Science, Faculty of Biological Sciences, University of Leeds, Leeds, UK
[b] Rheumatology & Rehabilitation Research Unit, University of Leeds, Leeds, UK
[c] Department of Rheumatology, Dewsbury District Hospital, Mid-Yorkshire NHS Trust, Dewsbury, UK

ARTICLE INFO

Article history:
Received 25 July 2014
Revised 11 March 2015
Accepted 5 April 2015
Available online 12 April 2015

Edited by Robert Recker

Keywords:
Cancellous bone disconnection
Fracture site microarchitecture
Ageing vertebra
Ageing femur
Osteoporosis
Osteoarthritis

ABSTRACT

Trabecular bone disconnection is an independent factor in age-related skeletal failure where real termini (ReTm; rare in youth) may cause weakness disproportionate to tissue loss, yet their structural contribution at vulnerable locations remains uncertain. ReTm (previously recorded at the iliac crest) were mapped in "normal" aged vertebral bodies (T11–L5 autopsy; 20 females, 10 males) and corresponding proximal femora (autopsy; 10 females). Results were compared with biomechanically failed femora from orthopaedic subjects aged >58 yr (osteoporosis OP, 10 females; osteoarthritis OA, 10 females). A novel direct 2D/3D histological method was applied to large, thick (300 μm) slices superficially silver-stained to separate ReTm (unstained) from apparent termini (planar artefacts, brown). Light microscope field co-ordinates enabled ReTm mapping and statistical testing relative to i) sex, ii) tissue sector and iii) slicing plane. In men ReTm populations were small and random while in women they were large and sector-specific. In vertebrae they clustered anterior/superior being rare posterior/inferior; in the femoral head they concentrated distal/superior and also near the fovea, being fewer distal/inferior. A distribution polarity was evident with 100% more ReTm observed transversely (i.e., on tensile-related cross struts) than longitudinally (i.e., on compression-related vertical struts). Their numbers rose in OP (BV/TV < 14%, microCT) and in OA (BV/TV > 14%), remaining polarised and sector-specific in OP only. Comparative experimentation by marrow elution of an OP animal model demonstrated "floating segments" as a possible outcome. Conclusions were supported statistically that trabecular disconnection "hotspots" at vulnerable locations are sex- and sector-specific, mainly transaxial, and subject to disease modulation.

Introduction

Bone mass is a major factor in sustaining mobility in ageing populations and can be measured with precision. At the same time, reports continue to suggest that skeletal strength in the elderly is influenced by trabecular architectural deterioration, which may be independent of bone quantity [1,2], making future fracture prediction at vulnerable sites more difficult. A range of mathematically diverse 2- and 3-dimensional histological procedures (see references [3,4]) has been applied extensively in the literature to determine microarchitectural aspects of cancellous bone behaviour [for example [5–9]]. Despite the attention, the assessment of cancellous disconnection remains a histological challenge [10], especially as its structural impact can exceed its comparatively modest appearance. To measure the variable directly, rather than indirectly (as is commonly the case) a novel histological technique [11–13] was developed and statistically validated for identifying and separating "real" trabecular termini (ReTm; a direct index of structural disconnection) from "apparent" trabecular termini (planar artefacts of 2-dimensional imaging). This research method was applied previously to iliac bone biopsies (the traditional skeletally representative bone biopsy site) from two groups of age-matched postmenopausal women with and without vertebral crush fractures despite the groups having an identical bone mass (histologically and by absorptiometry). Established methods consistently failed to identify a significant structural distinction in trabeculation between these two mass-matched groups [12], while the relatively simple new direct method was sufficiently sensitive to discriminate a mass-independent deterioration in the fracture-prone subjects as a significantly raised number of real trabecular termini [13]. This method suggested that trabecular termini are not always transitory projections, but may persist indefinitely as redundant segments of the cancellous network, continuing to contribute to the bone mass when no longer apparently relevant to its structural function.

* Corresponding author at: School of Biomedical Science, Faculty of Biological Sciences, Garstang Building, University of Leeds, Leeds LS2 9JT, UK.
E-mail addresses: j.e.aaron@leeds.ac.uk (J.E. Aaron), E.M.A.Hensor@leeds.ac.uk (E.M.A. Hensor), Lesley.hordon@midyorks.nhs.uk (L.D. Hordon).

http://dx.doi.org/10.1016/j.bone.2015.04.009

The following investigation extrapolates from the previous iliac crest ReTm histomorphometry described above and aims to examine directly the incidence and potential impact of network severance at two cancellous bone locations known to be particularly vulnerable to minimal trauma fractures. The objectives are to *i*) establish if "real" termini (ReTm) are evident in the normal ageing vertebral spine in women compared to men; *ii*) compare their distribution pattern in the spine and corresponding normal ageing hip; *iii*) compare the effect of age-related disease on ReTm distribution in the hip with reference to osteoporosis and osteoarthritis as histopathogenetically and mechanically contrasting conditions; and *iv*) evaluate experimentally the structural outcome of a localized multiplicity of ReTm by reference to an atrophic animal femoral model using marrow extraction and density fractionation procedures.

Material and methods

Specimens

Vertebral bodies were separated by division of the pedicle and removed as available in accordance with the Human Tissues Act from the lower thoracic (T11–12) and lumbar (L1–5) spine of female and male cadavers aged 75–89 yr (mean 81 yr) donated for anatomy dissection to the University of Leeds, and with no history of bone disease or malignancy (typically congestive heart failure and bronchopneumonia as cause of death) and separating any with external evidence of deformity suggestive of crush fracture [14]. Specimens (Table 1) comprised 20 vertebral bodies from 5 female subjects, and for comparison 10 vertebral bodies from 4 males. In addition were 10 cadaveric "normal" female femoral heads from these subjects. Further femoral heads were kindly provided by the surgeons of the Orthopaedic Department of Dewsbury District Hospital Mid-Yorkshire NHS Trust as surgical discards following ethical approval and informed patient consent from fracture subjects (osteoporosis OP; aged 58–95 yr, mean 76 yr) and non-fracture subjects (osteoarthritis OA; aged 60–78 yr, mean 71 yr).

Preparation

The undecalcified specimens preserved in 70% ethanol were dehydrated in absolute alcohol. After immersion in ethanol:chloroform (1 day) and brief xylene treatment they were embedded intact in methylmethacrylate (with dibutylphthalate plasticizer and benzoyl peroxide catalyst; see [4,6] for details), the permeation and polymerisation commencing under vacuum for 15 min to withdraw trapped air bubbles and proceeding in a water bath at 25 °C to control the exothermic reaction. The process took 4 weeks for these exceptionally large histological specimens (subdivision prior to embedding risked microdamage). The plastic-embedded blocks were bisected sagittally, using the fundus and *Ligamentum teres* as a landmark in the case of the proximal femora which had been detached transcervically or intertrochanterically. Sectioning followed using a Microslice 2 (Metals Research Ltd, Cambridge) equipped with a diamond-impregnated, water-cooled rotating blade to collect slices 300 μm thick (confirmed with a Mitutoyo micrometre, accurate to 1 μm, to enable the volumetric incidence of ReTm to be calculated). Some specimens were serially sliced throughout (generating >30 slices), each slice taking 15–30 min. However, it was more manageable to collect slices every 2 mm, amounting to 7 large slices per specimen. While some bisected specimens were sliced coronally (i.e., vertically) only, other pairs were separated and of these one half sliced vertically and the other transversely. These latter comprised 10 vertebrae from 4 females (1 each of T12, L1 and L2; two each of L3, L4; three of L5) and 10 vertebrae from 4 males (2 of T11; one each of T12 and L1; two of L4; four of L5). To differentiate real termini from planar artefacts upper and lower surfaces of the thick slice were stained according to the method of Shore et al. [11] and Aaron et al. [13] (see also [4]) using the von Kossa silver stain for bone mineral and immersing the slices in 2% silver nitrate solution for 30 min, enabling the brown colour of the silver nitrate to develop under a 60 watt light bulb at 20 cm distance. This stained only the superficial exposed bone matrix (and not that contained within the depth of the slice). It was followed by rinsing, blotting and clamping between polythene-lined glass microscope slides to flatten for 24 h prior to mounting in XAM organic medium.

Table 1
Vertebrae from elderly female (F) and male (M) autopsy (7 sagittal slices cut from each).

Source	Number	Spine level
Subject 1 F	7 vertebrae	T11, T12, L1, L2, L3, L4, L5
Subject 2 F	7 vertebrae	T11, T12, L1, L2, L3, L4, L5
Subject 3 F	3 vertebrae	L1, L4, L5
Subject 4 F	2 vertebrae	L4. L5
Subject 5 F	1 vertebra	L4
Subject 1 M	4 vertebrae	L5
Subject 2 M	3 vertebrae	T11, L4, L5
Subject 3 M	2 vertebrae	L4, L5
Subject 4 M	1 vertebra	L5

Histomorphometry

Paired co-ordinates defining the position of the cortical endosteum were recorded under a Zeiss photomicroscope using the graduated X- and Y-axes of the microscope stage micrometre to plot the outline of the specimen (the 0, 0 setting provided a fixed reference point). To assist comprehensive scanning of the ReTm and to ensure that no area was analysed twice or overlooked, a transparent acetate grid with measurements proportional to the dimensions of each specimen was helpful and was constructed using Corel Draw (or Microsoft Word 2003) and placed on the slide underside (to minimise obstruction). With the area of interest centrally located the co-ordinates were recorded for each ReTm at ×80 magnification, the analysis time averaging 20 min per slice. Representative digital photographs were taken using a Canon Powershot G5 camera and laptop computer and a proportion of the thick slices was scanned in a Micro-CT 80 scanner (Scanco, Switzerland [15]) to provide an automated measure of the relative cancellous bone volume BV/TV% for reference.

Data analysis

For histological analysis of the vertebral bodies each slice was divided into nine equal sectors defined by their position on the X-axis (anterior, medial or posterior) and Y-axis (upper, central, lower), each axis category being one third of the maximum. In this way the number of ReTm was determined for each sector. Similarly for the proximal femora each slice was divided into six equal sectors defined by their position on the X-axis (distal, medial and proximal) and Y-axis (superolateral, inferolateral). Numbers of ReTm were summated across slices within each spatial sector. To identify clustering, the ReTm number was compared among different sectors of the vertebra or femoral head using the Friedman test followed by Dunn–Bonferroni pairwise tests for differences between sectors; the ReTm number was compared between anterior and posterior regions of the vertebra using Student's paired t-test. Also conducted were mixed between-within analyses comparing spatial trends between sexes or disease groups using repeated measures ANOVA (RM-ANOVA), reporting Wilks' Lambda for within-subjects effects if the assumption of sphericity was violated, and using Bonferroni adjustment where necessary for between-group comparisons. Non-parametric analysis was used to identify clustering of ReTm in sectors on the X- and Y-axes because the data were skewed. Statistical tests were only performed in the spine at particular levels (L4, L5) to include just one observation per subject, thus satisfying the assumption that observations were independent. In this statistically small, unpowered study results were provided

from inferential tests on an exploratory, rather than confirmatory basis. All analyses were performed in SPSS version 21.0.0.1 (IBM).

Experimental rodent model of cancellous disconnection

Animal models provide the means of experimental testing for those validating human bone behaviour. The ex-breeder female rat constitutes an inexpensive model of human cancellous bone atrophy for comparison with the intact spongiosa of age-matched virgins [16]. Wistars routinely culled after three successive breeding cycles were used to investigate microarchitectural detachment by, on the one hand, established histology and, on the other, marrow elution. The usual histological application of elution is to improve cancellous imaging by removing the masking effect of the fatty marrow as a disposable extract. In the present context the traditionally discarded extract was of special interest for any containment of dense elements also descending. Left and right femora were dissected from 7 ex-breeder animals, cleared of adherent tissue and sharply bisected across the mid-shaft where trabeculae tend to be absent and the cortex wide (minimising the production of particulate bone "dust"). Thick slice histology (2.2 above) was performed on the untreated left limb to confirm if ReTm were indeed a feature of rodent bone. The corresponding right femora were used for marrow extraction by heating to 55 °C in 0.75 M NaOH for 2 h (modified from Odgaard et al., *J. Microsc. 159, 335,* 1990, cited by Aaron & Shore [4]). The eluent was centrifuged to separate any heavy fraction for examination by polarised light microscopy, enabling detached network segments to be identified by lamellar birefringence and osteocytes, and comparison made with similarly treated control virgin rats.

Results

At both the normal elderly human spine and hip light microscopy of the slices confirmed thin cortical envelopes and the sporadic incidence of unstained ReTm (Figs. 1a–c), with occasional bony islands. In profile the ReTm were either irregular and fragmented or, more commonly, smooth and rounded as long, finger-like or short, stump-like projections, suggestive of a developmental sequence. The contrasting histopathology of OP and of OA is well-documented in the literature. Macroscopically in OP the uncalcified articular cartilage layer was thick and regular with reduced subchondral bone (BV/TV women 11% ± 4SD c.f. normal elderly 17% ± 5SD), while in OA the partially calcified articular cartilage layer was grossly uneven with irregularly hypertrophic subchondral bone (BV/TV mean 22% ± 6SD). A special characteristic of OA, uncommon elsewhere, was discrete microcallus [17], implying a spontaneous repair response to a proportion of trabecular severance (Fig. 1d).

Vertebral ReTm

A typical ReTm map is shown in Fig. 2. The populations of ReTm in the vertebral bodies were assessed in relation to i) anterior/posterior distribution with respect to sex; ii) clustering in defined sectors with respect to women only; and iii) planar disposition with respect to sex.

Anterior versus posterior: female and male spine

The number of ReTm was counted in the anterior and posterior regions of the 7 slices from each of the 20 vertebral bodies from women (Table 2) and they appeared to be more frequent in the anterior region

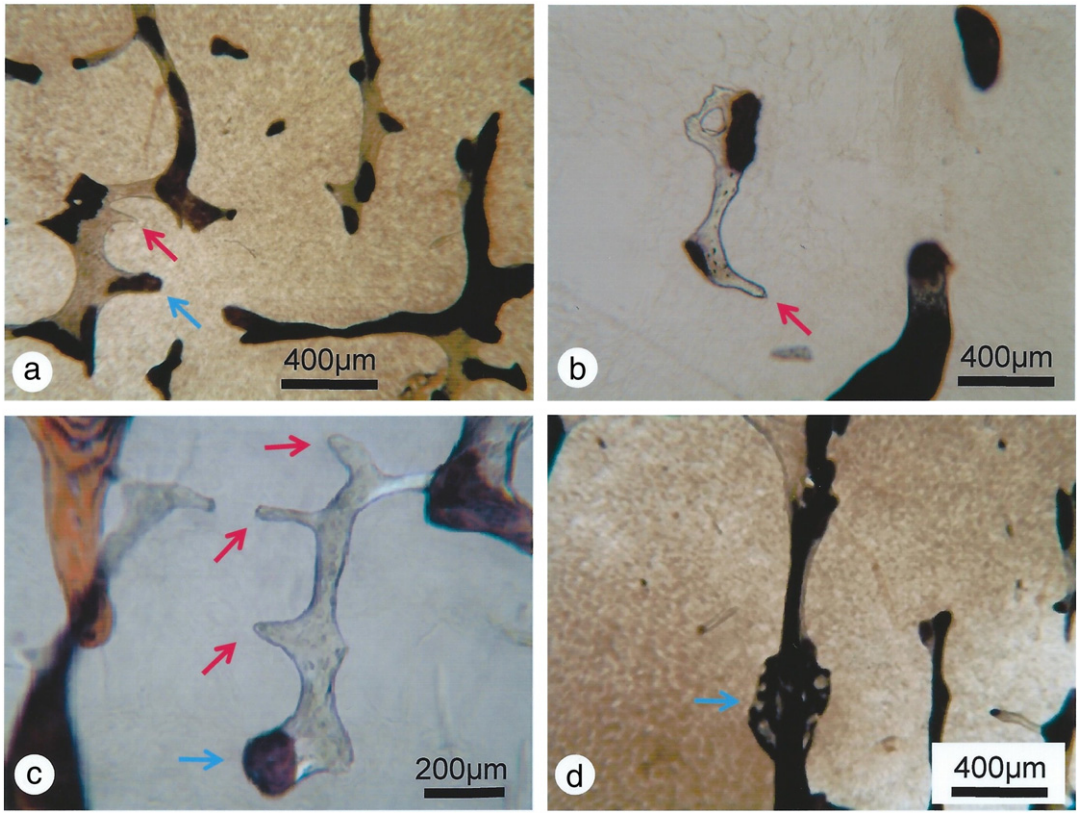

Fig. 1. Photomicrographs showing trabecular disconnection as real termini (ReTm) in surface-stained thick (300 μm) slices of elderly human vertebral body. a–b) Examples of ReTm (unstained, red arrows) and apparent terminus (dark brown stained planar artefact, blue arrow). c) A series of ReTm (red arrows) on parallel horizontal trabeculae and an apparent terminus below (blue arrow). d) Microcallus repair (blue arrow) on a vertical trabecula. Plastic-embedded, von Kossa silver stain, partly polarised light. Scale bars as indicated.

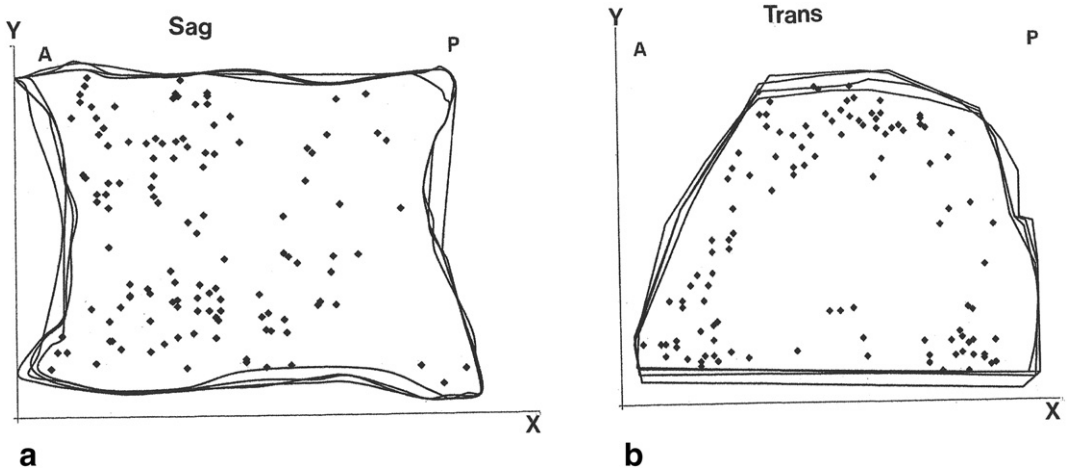

Fig. 2. Typical vertebral real terminus maps from a normal elderly woman, showing the data-constructed cortical enclosure of populations of ReTm in four superimposed thick slices. Microscope stage X-axis and Y-axis coordinates in a) sagittal (sag) plane and b) transverse (trans) plane; anterior (A) and posterior (P) vertebral face.

of all the vertebrae examined. This could be tested statistically at spine level L4 [n = 5; mean ReTm anterior 30.8 c.f. posterior 15.4; difference (95% CI) 15.4 (8.7, 22.1), p = 0.003] and at L5 [n = 4; mean ReTm anterior 36.0 c.f. posterior 13.0; difference (95% CI) 23.0 (9.1, 36.9), paired t-test p = 0.013]. When repeated in the 7 slices from each of the 10 male vertebral bodies counted separately as anterior and posterior (Table 2) the total number of ReTm was fewer than in women with little apparent anterior–posterior difference. This distinction in spatial trend between the sexes could be tested statistically at spine level L5 [n = 4; mean ReTm anterior 17.5 c.f. posterior 13.8; difference (95% CI) 3.8 (1.7, 5.8); Wilks' Lambda for interaction between sex and anterior–posterior difference = 0.24, p = 0.005].

Scattered versus clustered: female spine

Because in men in 3.1.1 above there were fewer ReTm and they were apparently random in distribution, examination of any aggregation tendency was confined to women. The combined data from the above 20 vertebrae was analysed to determine whether the distribution of ReTm was heterogeneous throughout the 9 sectors as defined in each sagittal slice (Fig. 3). There was apparently both a trend towards a greater number of ReTm in the anterior of the vertebral body and also a trend towards a greater number in the upper part of the vertebra (Fig. 4). Differences between the mean ranks computed for pairs of sectors illustrated that each of the anterior sectors (1, 4, 7) and the upper medial sector (2) had more ReTm than the lower posterior sector (9). The upper and central anterior sectors (1, 4) had more ReTm than the upper and central posterior (3, 6) and lower medial (8) sectors. This could be formally tested at spine level L4; despite the small number of vertebrae included (n = 5), the results indicated that there were differences among the various sectors of the vertebrae (Friedman test n = 5, Chi-square = 26.89, df = 8, p = 0.001; see online supplementary Table S1 for descriptive data). While each of the differences highlighted above was significant at $p < 0.05$ in unadjusted analyses at L4, following adjustment for multiple comparisons in this small group only the

Table 2
Comparison of ReTm number, anterior versus posterior, in vertebral bodies of elderly females (F) and males (M), each prepared as 7 sagittal slices (individually 20 mm × 30 mm × 0.3 mm, average cancellous volume 200 mm^3).

Subject	Anterior half:posterior half (total count)						
	T11	T12	L1	L2	L3	L4	L5
S1 F	70:43	70:45	80:28	59:27	63:43	50:34	55:30
S2 F	49:22	51:30	63:36	30:13	51:30	24:05	20:09
S3 F	–	43:31	–	–		22:08	25:01
S4 F	–	–	–	–	–	29:08	44:12
S5 F	–	–	–	–	–	29:22	–
[*Overall F mean ReTm number A:P 6.6:3.4 per 100 mm^3 spongy bone*]							
S1 M	25:24	42:38	23:21	–	–	–	16:12
S2 M	38:39	–	–	–	–	30:25	18:16
S3 M	–	–	–	–	–	17:20	17:12
S4 M	–	–	–	–	–	–	19:15
[*Overall M mean ReTm number A:P 3.5:3.2 per 100 mm^3 spongy bone*]							

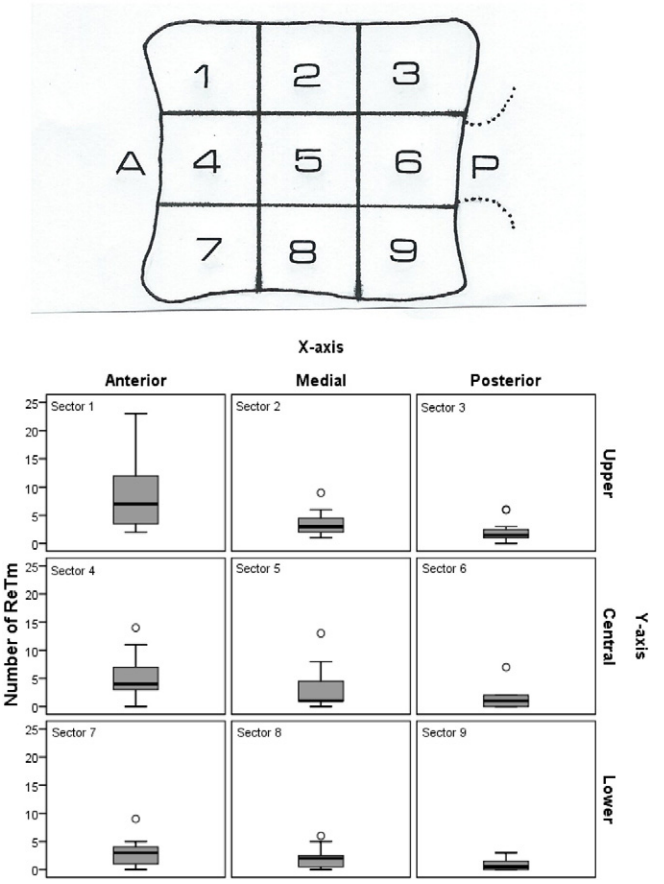

Fig. 3. Combined real terminus number [median (inter-quartile range) for 20 sagittal vertebrae from 5 elderly females, 7 slices each] mapped relative to nine equal regional sectors (top diagram, anterior A, posterior P).

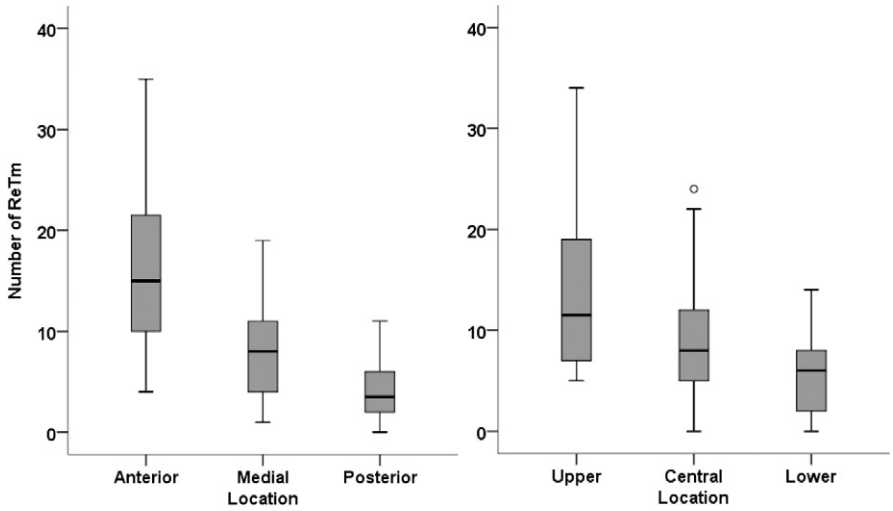

Fig. 4. Box and whisker plots of real terminus (ReTm) number plotted according to summative regional sectors in 20 sagittal vertebrae from 5 elderly females.

difference between the upper anterior and lower posterior sectors remained significant (standardised Dunn–Bonferroni test statistic 3.64, $p = 0.010$).

Sagittal versus transverse: female and male spine

The number of ReTm was counted and compared in 5 sagittal (i.e., vertical) and 5 corresponding transverse slices from 10 vertebrae of 4 females and from 10 of 4 males. Comparison of BV/TV with axial plane in the 10 randomly selected pairs found no substantive difference (14% c.f. 13%). Repeated-measures ANOVA (RM-ANOVA) at L5 (female $n = 4$, male $n = 4$) detected a significant interaction between plane and sex (Wilks' Lambda $= 0.14$, $p = 0.003$), indicating that the difference between the sagittal and transverse planes was not constant across the sexes, and vice versa. Examination of the descriptive data for all 20 vertebrae showed that while in females there were more ReTm in the transverse plane than in the sagittal plane [mean (SD) 64.8 (23.2) vs. 30.3 (19.6)], there was no substantive difference in the number of ReTm between the two planes in vertebrae from males [21.3 (9.6) vs. 16.6 (5.2)] (Fig. 5). It follows that while a greater number of ReTm were recorded in females than in males in both planes, the greatest difference was observed in the transverse plane.

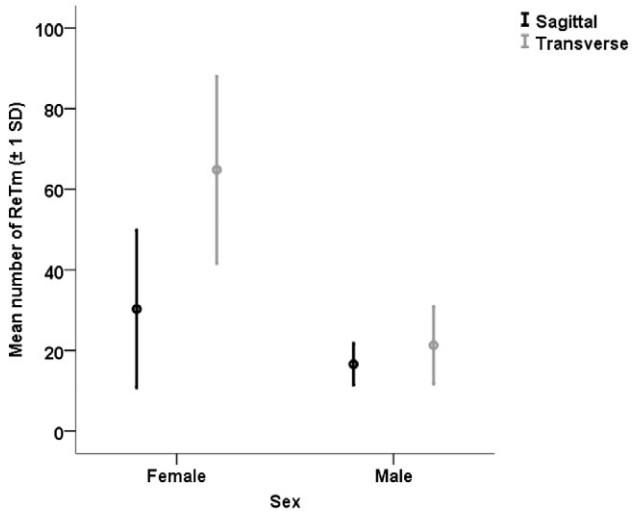

Fig. 5. Planar comparison of vertebral real terminus (ReTm) number in elderly females and males. In women (10 vertebrae from 4 subjects, 5 slices each) the total overall descriptive data shows more ReTm throughout the transverse plane than the sagittal plane. In men (10 vertebrae from 4 subjects, 5 slices each) there were fewer ReTm and no substantive difference between planes.

Femoral ReTm

Typical ReTm maps are shown in Fig. 6. Because the results above (3.1.1) suggest that ReTm are a factor of more significance in women than in men thereby supporting previous evidence at the iliac crest [6, 13], the following ReTm analysis was confined to female femoral heads according to i) clustering in defined sectors and the comparative effect on this of OP and OA; ii) planar disposition and the comparative effect on this of OP and OA; and iii) an experimental animal model of trabecular network segmentation.

Scattered versus clustered: female hip (normal, OP, OA)

Numbers were counted in 7 thick sagittal slices from the femoral heads of the 10 subjects in each cohort. Repeated measures ANOVA was used to determine whether the three groups (normal, OP, OA) differed in the numbers of ReTm identified, and in the pattern of ReTm distribution across the 6 arbitrary sectors (Fig. 7) of the femoral head. A significant interaction was detected between sector and group (Wilks' Lambda $= 0.42$, $p = 0.018$), indicating that the differences in the number of ReTm between the sectors were not constant across all groups (Fig. 8). Separate analyses in each group indicated that the number of ReTm differed among the sectors in the normal/autopsy group (Wilks' Lambda 0.42, $p = 0.002$) and OP group ($F = 6.82$, $p < 0.001$), but did not differ in the OA group ($F = 1.18$, $p = 0.336$). Bonferroni-corrected post-hoc tests indicated that in patients with OP the mean number of ReTm in sector 1 was higher than in sectors 2, 3 and 5 but did not differ from sectors 4 and 6. The same pattern (although with fewer ReTm overall) was observed in the normal subjects, whereas in OA the sectors did not differ substantively. Thus sectors 2, 3 and 5 of OA were comparable to OP (and had more ReTm than normal subjects), while sector 1 of OA tended to have fewer ReTm than the other groups (Table S2, online supplementary).

Sagittal versus transverse: female hip (normal, OP, OA)

Five randomly selected sagittal slices above were compared with 5 transverse slices cut from the remainder of the plastic-embedded tissue block. There was no substantive difference in comparison of BV/TV with axial plane in any group (normal 16% c.f. 15%; OP 11% c.f. 9%; OA 21% c.f. 20%). Mixed between-within repeated measures ANOVA was used to determine whether the three groups (normal, OP, OA) differed in the numbers of ReTm identified, and in the planar pattern of ReTm distribution. A significant interaction was detected between plane and group

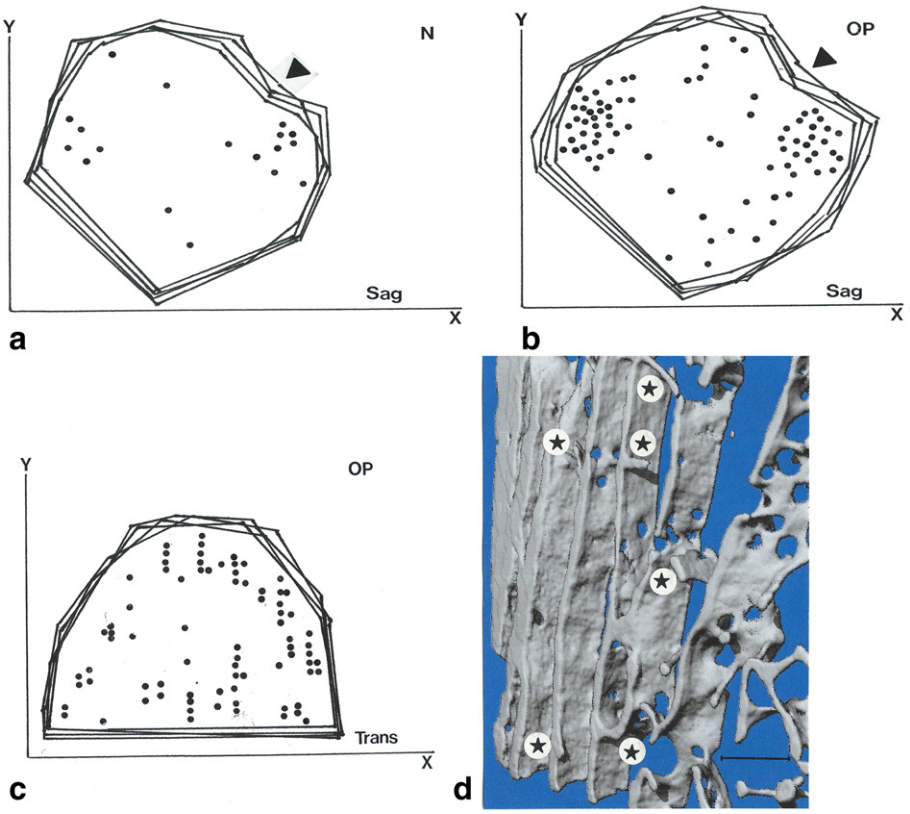

Fig. 6. Typical femoral head real terminus maps from elderly women, showing the data-constructed cortical enclosure of populations of ReTm in four superimposed thick slices (2 mm separation), and the tissue landmark fundus/*Ligamentum teres* region (arrowhead). Microscope stage X-axis and Y-axis coordinates in the sagittal (sag) planes of a) a normal (N) and b) an osteoporotic (OP) subject. c) Stage X- and Y-coordinates in the transverse (trans) plane of another (OP) subject, exemplifying ReTm populations in stacked groups that relate to d) parallel disconnected cross struts (*) between prominent linear arrays of vertical trabeculae, as observed by microCT. Scale bar 1 mm.

(Wilks' Lambda = 0.73, p = 0.015), indicating that the difference in the number of ReTm between the sagittal and transverse planes was not constant across all groups. Separate analyses in each group indicated that the number of ReTm differed significantly between the planes in each of the groups (normal/autopsy Wilks' Lambda 0.18, $p < 0.001$; osteoarthritis Wilks' Lambda 0.55, p = 0.024; osteoporosis Wilks' Lambda 0.22, $p < 0.001$). However, examination of the descriptive data revealed that the difference between the planes was largest in OP [transverse–sagittal mean difference (95% CI) 26.7 (16.2, 37.2)], and that normal subjects showed a similar disparity between the planes [19.1 (12.4, 25.8)], while in OA there was relatively little difference between the planes [9.8 (16.0, 18.0)], the number of ReTm in both planes being

Sector	Mean	95% Confidence Interval	
		Lower Bound	Upper Bound
1	6.8	5.7	8.0
2	3.8	2.9	4.7
3	2.5	1.7	3.3
4	4.0	3.0	5.1
5	3.5	2.6	4.3
6	6.3	4.8	7.8

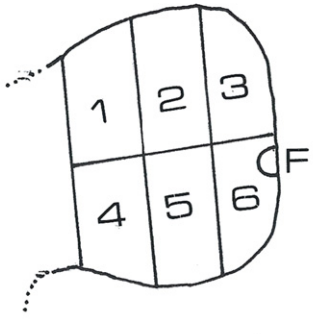

Significance	S2	S3	S4	S5	S6
S1	p=0.003	p<0.001	p=0.003	p<0.001	p=1.000
S2		p=0.371	p=1.000	p=1.000	p=0.180
S3			p=0.406	p=1.000	p=0.002
S4				p=1.000	p=0.105
S5					p=0.007

Fig. 7. Combined (30 elderly females, 7 slices each, normal and age-related disease) real terminus number mapped relative to six equal regional sectors in the sagittal proximal femur (diagram, with landmark fundus (F)). There were more ReTm in some sectors than others; sector 1 (S1) had significantly more than sectors 2 to 5 but similar to sector 6 (S6).

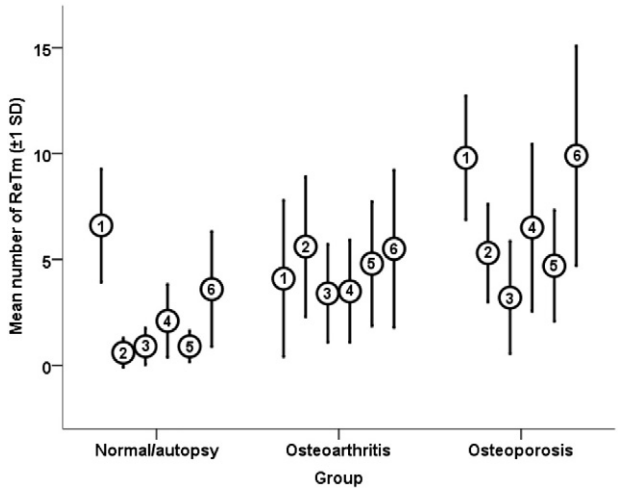

Fig. 8. Comparing the femoral head real terminus (ReTm) number and progressive increase with pathology in mapped sectors 1–6 in the three elderly female groups of "normal", OA and OP (ten subjects each), showing the similarity in relative sector distribution pattern between normal and OP, not evident in OA.

comparable to that in the femoral transverse plane of the normal subjects (Fig. 9).

Clustering ReTm and "floating" segmentation: animal model

The longitudinal femoral histology slices from ex-breeder rats with their intact marrow preserved (Fig. 10a) confirmed the presence of ReTm in an animal (Figs. 10b–c). Accompanying marrow elution was the descent of a dense fraction containing not only a few small bone shards and ovoid islands but also larger configurations of detached network "floating" segments with smooth rounded termini (Figs. 10d–f). In comparison femora from age-matched virgin rats showed no such features in the eluent, other than fine bone "dust" (Fig. 10e, inset).

Discussion

Youthful, well-interconnected bone withstands the normal range of forces that elderly disconnected bone cannot. The evidence above suggests that ReTm are optically visible histological hallmarks of disconnection within the cancellous network of the spine and hip. A postulated relationship between ReTm and structural weakness is based upon the mechanical principle of Euler's theorem. This states that severance of a cross strut between uprights reduces structural strength disproportionate to the small amount of material removed by a single event. Accordingly vertical trabecular strength is inversely proportional to length [18] and the removal of one stabilising horizontal trabecula to effectively double the distance between its neighbours reduces the resistance to bending forces fourfold, increasing buckling and microdamage. In this context are early descriptions by Atkinson [19] later confirmed [20,21] of preferential horizontal trabecular attrition in coronal aged vertebral bodies, to which have been added subsequent reports of low connectivity density and high marrow star volume, with zone-dependent changes [22–25] and irreversible trabecular perforations [26]. While pinpointing ReTm is complementary to these established variables, it also uniquely enables the creation of maps. These are of value in suggesting not only that women have significantly more ReTm than do men (as might be anticipated) but more especially that their distribution characteristics seem to differ fundamentally between the sexes and moreover to be susceptible to the imposition of contrasting conditions, such as OP and OA.

Individual ReTm can be classified histologically as rough or smooth, vertical or horizontal, primary or secondary, temporary or permanent. These properties may be sequential in that rough (in the minority) precedes the more common smooth, and primary cross strut disruption will increase secondary upright risk, while a temporary occurrence signals intrinsic healing. Mechanisms for ReTm genesis may include the hypogonadal, increased depth of osteoclastic resorption perforating thinning horizontal trabeculae [27–30], and to which may be added substructural trauma (microparticle slip and crystal fracture or discrete hydrolytic, matrix self-destruction (autoclasis) with multiple microfissuring) [31,32]. ReTm will relieve typically tension-loaded cross struts of the physical pressures mandatory for repair, with combined severance releasing ovoid bony islands [33–35]. In contrast, ReTm interrupting compression-loaded vertical trabeculae may continue to conduct sufficient compaction pressure to stimulate microcallus repair. At "hotspots" their numbers raise the likelihood of significant network segmentation into separate branched portions not easily detected by most methods, but apparently demonstrable in the marrow-eluted osteopoenic rat femur as 3-dimensional "floating" segments.

Sex-related "hotspots" and "coldspots" in the ageing spine

Vertebrae T11, T12 and L1, L4 are the most commonly fractured [36,37]. In explanation, intrinsic biomechanical accommodation of ageing vertebrae by the development of thicker or thinner or more widely spaced trabeculae may cause their misalignment and heterogeneity [21] which deflects from the central and mid-posterior regional axes of stress that normally transmit the greatest compressive strength [38]. In addition have been descriptions of more trabecular termini posteriorly by some authors (by peripheral quantitative computed tomographic density analysis, pQCT and by sectioning [25]) and conversely by others of minimal trabecular loss with age posteriorly (using high resolution microcomputed tomography [21]) and with deterioration most marked anteriorly [39]. An expanding ReTm population is consistent with increasing heterogeneity and chronic network dysfunction in women arising from an apparently predictable combination of a "hotspot" (anterior superior) and a "coldspot" (posterior inferior). Their comparative absence in men, where network integrity seems better retained and disconnection less focussed, is consistent with the contrasting patterns of cancellous bone loss previously reported between the ageing sexes [6], where generalized trabecular thinning rather than loss was the characteristic event in men.

It might be expected that the location of ReTm "hotspots" and "coldspots" would coincide with regions of relatively low and high trabecular bone density respectively. MicroCT scanning indicated no more

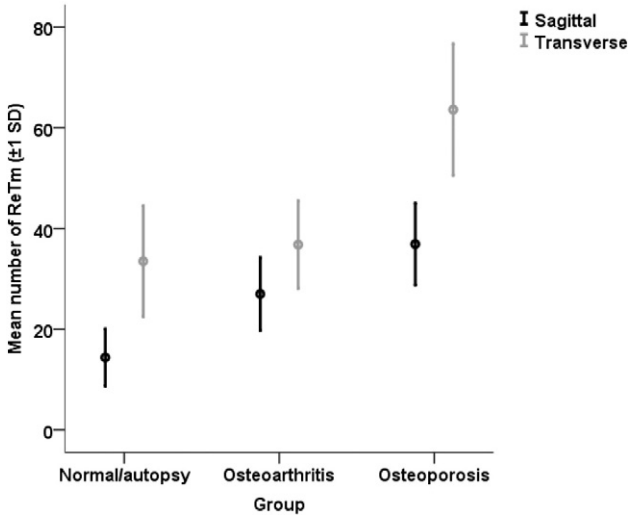

Fig. 9. Planar comparison of the femoral head real terminus (ReTm) number in the three elderly female groups of "normal", OP and OA (ten subjects each) showing a dominance in the transverse plane that was greatest in OP, followed by normal subjects, with little planar distinction in OA.

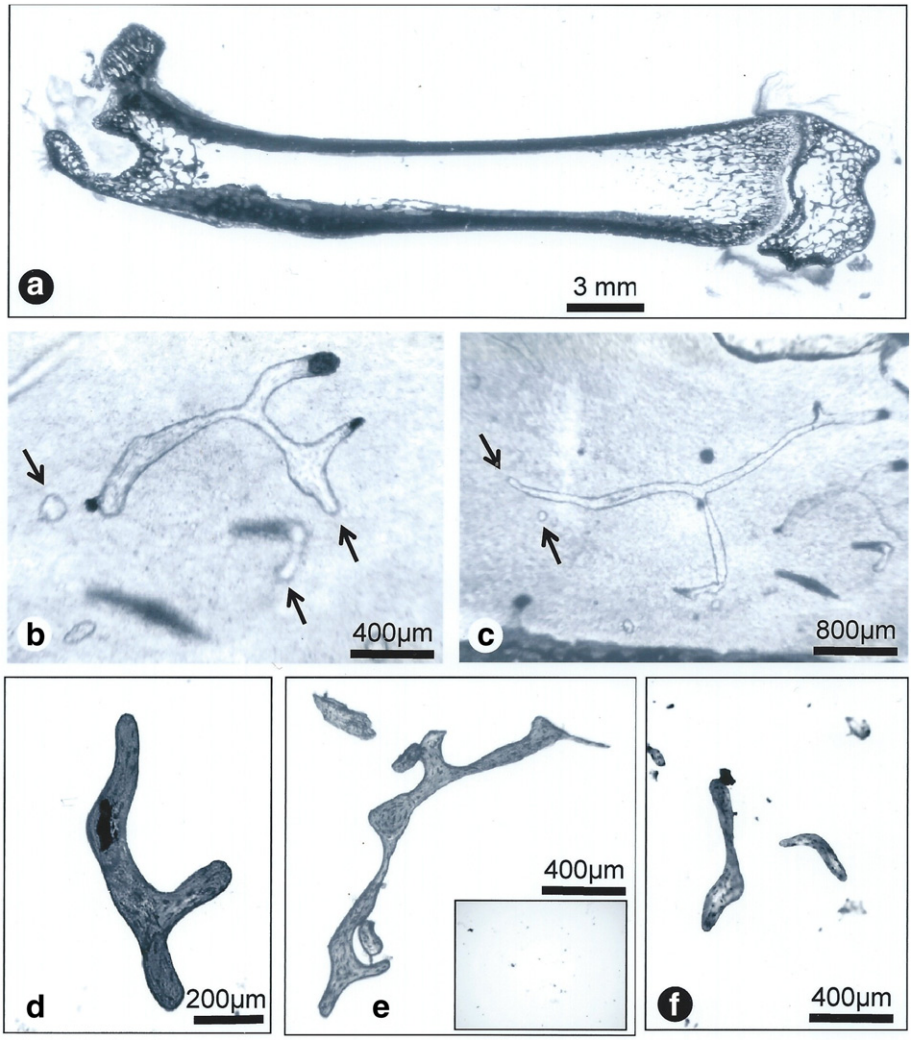

Fig. 10. Photomicrographs of trabecular disconnection (ReTm) and resultant "floating segments" in an osteopoenic rat model. a) Typical plastic-embedded entire femoral slice, 300 μm thick, superficial von Kossa stain, showing the LP panorama of atrophied spongiosa enclosed by cortical bone, with b–c) frequent ReTm and small rounded islands (unstained, arrowed). d–f). Examples of branched "floating" network segments collected in exbreeder marrow eluent, and absent (e—*inset*) from that of age-matched virgin controls, where fine bone "dust" was the only dense feature. Scale bars as indicated.

than an insignificant trend towards a lower BV/TV% in the former [40] consistent with a disproportionate number of ReTm in both locations and supporting previous reports of the independence of the two variables in iliac crest biopsies [13]. In a related pilot investigation comparing the relative advantages and potential of microCT scanning and histology for identifying ReTm it was noted that while microCT imaging supported the trabecular microarchitecture in thick slices, a proportion of apparent termini created by microtomy constituted false positives, i.e., microCT alone was not a reliable substitute for the histology (Aaron and Damien, unpublished).

"Hotspots" and "coldspots" in the ageing female hip

Consistent with the above observations is the description by van Rietbergen et al. [41] of "low-loaded bone" in the osteoporotic proximal femur suggestive of "the formation of loose trabecular ends." As in the vertebral body, so also in the femoral head increased cancellous heterogeneity is regarded as a fracture risk factor [42,43] and again the horizontal "tensile" trabeculae are apparently more expendable than the vertical "compressive" ones, those vertically receiving the stress of gait and heel-strike being conserved [44] at the expense of the rest. The femoral *Ligamentum teres* (*L. teres*) is a useful mapping landmark. The region at and immediately inferior to this unique insertion from which periosteal Sharpey's fibres permeate into the bony tissue [45] contains few or no cancellous structures, for which various explanations have been made. However, most significantly, the insertion is located at the boundary between the well recognized compressive (superior) and tensile (inferior) trabecular groupings identified by Singh et al. [46]. The occurrence of the first hip "hotspot" (inferior to *L. teres*) apparently coincides with the so-called tensile array, as is also the case for the second hip "hotspot" (distal superior). Conversely, a first "coldspot" (superior to *L. teres*) coincides with the apparent compressive trabecular array, as also does a second "coldspot" (distal inferior).

The relationship between OP and OA as common disabling diseases of ageing is generally considered to be controversial. However, the contrasting histopathogenic, substructural and biomechanical properties of classical OP and OA femoral heads seem undeniable and the two conditions tend to be mutually exclusive, at least at the outset [47–50]. The evidence above adds to the histological distinction. In the skeletally atrophied OP women the raised ReTm number supported previous observations on associated fragility and fracture [13]. In addition they showed a marked adherence to and consolidation of the ReTm clustering and polarity of the "normal" elderly subjects. In contrast, the raised ReTm number in the hypertrophied OA women resembled the male distribution pattern of randomness and nonpolarity. Influential factors distinguishing this group of women may include strong microcallus

intervention and a tendency towards subchondral sclerosis as highly stressed soft joint tissues harden in concert with change in the trabecular dynamics. The overall raised ReTm number common to the conditions of relatively high (OA) and low (OP) trabecular bone volume again supported the independence of the two histological variables. In so doing, it may suggest an advantage in the ratio *ReTm*:*BV/TV* to accommodate the raised incidence of ReTm in one group (OA) not characterised by fracture from another group (OP) that is. It follows that the ratio *ReTm*:*BV/TV* is significantly higher in OP than OA consistent with the fragility and fracture predisposition of the one and not the other.

However, there is room for caution in the interpretation of both 4.1 and 4.2 in relation to clinical fracture. In particular the histological evidence is based upon static and single time point assessment of a process that is time — or stress-dependent. On the other hand, the anterior vertebral ReTm "hotspot" seems especially consistent with reports of wedge fractures being the most common type [51], apparently constituting 69% [52] of vertebral fractures with age. Similarly "hotspot" location in the hip may directly or indirectly destabilise the arching tension lines of prominent transcervical to intertrochanteric trabecular arrays which traverse the entire region. In order to consolidate the proposed ReTm "hotspot" event (and acknowledging the associated risk of becoming experimentally cumbersome) a diversity of interrelated material (2 locations, 2 disease states, 2 species) was combined making the investigation a large one in practical histological terms. Statistically, it was governed by the availability of appropriate human material, which is invariably insufficient and from that perspective each aspect could be considered as small and exploratory; thus for analysis at the spine sample size had to be reduced to include just one observation per subject. In the spine it was opted not to perform statistical tests within subgroups following the detection of an interaction in favour of presenting descriptive data; in consequence their repetition in a larger sample is required to confirm the findings. For this reason there is in readiness the future expansion of the manual mapping method above by means of a spatial computer-assisted procedure combining in-house software and microCT imaging [[40], and in preparation], which will expedite larger group analysis than was possible here. Finally, unlike the main aspects, the inclusion of an animal model of atrophy may furnish those wanting to experiment with an essential controlled and dynamic approach that potentially may relate the ReTm phenomenon and ultimate "floating segment" concept to skeletal strength in a manner less theoretical than either Euler's theorem or the various theories of load effects on bone [53] such as the hypothetical "mechanostat" of Frost [54].

Conclusions

Reference to ReTm and consequent cancellous network segmentation may provide insight into elderly bone properties and behaviour. Thus the phenomenon of ReTm accumulation into discrete "hotspots" i) characterises women more than men, ii) apparently relates more to tension than compression, iii) seems to be accentuated by OP and diffused by OA, iv) may pre-empt collapse as networks segment and strength wanes disproportionate to tissue loss, and v) seems to arise in locations that are predictable. Although disconnection mapping is primarily a fundamental research tool enabling separation of tissue destined for "floating" segmentation from the rest, there may be useful applications. First clinically, ReTm may guide general understanding towards better diagnosis and screening, with insight into therapeutic restitution by reconnection. Second, in orthopaedics the "hotspots" may enable more effective targeting of putative loci of weakness for prophylactic fillers and other agents. Third, their inclusion may refine computer-assisted simulation and finite element modelling systems. Fourth, insight might be gained from the individual trabecular network segments after marrow elution, perhaps exposing inherent substructural characteristics that define their particular status (for example, the disappearance of permeating periosteal Sharpey's fibres [45]).

Acknowledgments

JEA, LDH and PAS are grateful to Action Medical Research and the HSA Charitable Trust for sequential project support for nine years on this and interrelated aspects. MI (orthopaedic surgeon) had a Visiting Fellowship from the University of Sapporo, Japan. We are indebted to Mr T. McAndrew, School of Biomedical Sciences, University of Leeds for guidance on coordinate mapping to associated postgraduate and undergraduate research students, in particular are S.A. Armstrong for Fig. 2, Damian for Fig. 6d, A.K. Missick and C. Zang for extensive analysis, together with J.O. Beardsell, K.L. Brown, L.P. Bubb, F. Carr, R. Hazeldene, F. McClelland, R. Payne, M. Thomas, N.E. Waylen and H. Welbourn. Figure formatting assistance was from Dr R. Shore, while an EPSRC Challenging Engineering programme for spine-related projects provided an interdisciplinary context. Dedicated to Profs P.J. Meunier (Lyons) and J.A. Kanis (Sheffield) for early and later encouragement.

Appendix A. Supplementary data

Supplementary data to this article can be found online at http://dx.doi.org/10.1016/j.bone.2015.04.009.

References

[1] McDonnell P, McHugh PE, O'Mahoney DO. Vertebral osteoporosis and trabecular bone quality. Ann Biomed Eng 2006;35:170–89.
[2] Ott S. When bone mass fails to predict bone failure. Calcif Tissue Int 1993;53(S1):S7–S13.
[3] Compston JE. Connectivity of cancellous bone: assessment and mechanical implications. Bone 1994;15:463–6.
[4] Aaron JE, Shore PA. Histomorphometry. In: Langton CM, Njeh CF, editors. The physical measurement of bone. Bristol, Philadelphia: Institute of Physics Publishing; 2004. p. 185–224.
[5] Tabor Z, Rokila E. Comparison of trabecular bone architecture in young and old bones. Med Phys 2000;27:1165–73.
[6] Aaron JE, Makins NB, Sagreiya K. The microanatomy of trabecular bone loss in normal aging men and women. Clin Orthop Relat Res 1987;215:260–71.
[7] Aaron JE, Skerry TM. Intramembranous trabecular generation in normal bone. Bone Miner 1992;17:399–413.
[8] Carter DH, Sloan P, Aaron JE. Trabecular generation de novo: a morphological and immunohistochemical study of primary ossification in the human femoral anlagen. Anat Embryol 1992;186:229–40.
[9] Aaron JE, de Vernejoul M-C, Kanis JA. Bone hypertrophy and trabecular generation in Paget's disease and in fluoride-treated osteoporosis. Bone Miner 1992;17:399–413.
[10] Odgaard A, Gundersen HJG. Quantification of connectivity in cancellous bone with special emphasis on 3-D reconstruction. Bone 1993;14:173–82.
[11] Shore PA, Shore RC, Aaron JE. A three-dimensional histological method for direct determination of the number of trabecular termini in cancellous bone. Biotech Histochem 2000;75:183–92.
[12] Hordon LD, Raisi M, Aaron JE, Paxton SK, Beneton M, Kanis JA. Trabecular architecture in women and men of similar bone mass with and without vertebral fracture: I. Two dimensional histology. Bone 2000;27:271–6.
[13] Aaron JE, Shore PA, Shore RC, Kanis JA. Trabecular architecture in women and men of similar bone mass with and without vertebral fracture: II. Three dimensional histology. Bone 2000;27:277–82.
[14] Genant HK, Wu CY, van Kuijke KC, Nevitt MC. Vertebral fracture assessment using a semiquantitative technique. J Bone Miner Res 1993;8:1137–48.
[15] Hordon LD, Itoda M, Shore PA, Shore RC, Heald M, Brown M, Kanis JA, Rodan GA, Aaron JE. Preservation of thoracic spine microarchitecture by alendronate: comparison of histology and microCT. Bone 2006;38:444–9.
[16] Shahtaheri MS, Johnson DR, Paxton SK, Aaron JE. The impact of reproduction on the mammalian skeleton. J Anat 1999;194:407–21.
[17] Vernon-Roberts B, Pirrie CJ. Healing trabecular microfractures in the bodies of lumbar vertebrae. Ann Rheum 1973;32:406–12.
[18] Davison KS, Siminoski K, Adach JD, Hanley DA, Goltzman D, Hodsman AB, et al. Bone strength: the whole is greater than the sum of its parts. Semin Arthritis Rheum 2006;36:22–31.
[19] Atkinson PJ. Variation in trabecular structure of vertebrae with age. Calcif Tissue Res 1967;1:24–32.
[20] Gong H, Zhang M, Yeung HY, Qin L. Regional variations in microstructural properties of vertebral trabeculae with ageing. J Bone Miner Metab 2005;23:174–80.
[21] Thomsen JS, Ebbesen EN, Li Mosekilde. Age-related differences between thinning of horizontal and vertical trabeculae in human lumbar bone as assessed by a new computerized method. Bone 2002;31:136–42.

[22] Thomsen ES, Ebbesen EN, Li Mosekilde. Zone-dependent changes in human vertebral trabecular bone: clinical implications. Bone 2002;30:664–9.
[23] Thomsen ES, Ebbesen EN, Li Mosekilde. Predicting human vertebral bone strength by vertebral static histomorphometry. Bone 2002;30:502–8.
[24] Banse X, Devogelaer JP, Munting E, Delloy C, Cornu O, Grynpas M. Inhomogeneity of human cancellous bone: systemic density and structure patterns inside the vertebral body. Bone 2001;28:563–71.
[25] Banse X, Devogelaer JP, Grynpas M. Patient-specific microarchitecture of vertebral cancellous bone: a peripheral quantitative computed tomographic and histological study. Bone 2002;30:829–35.
[26] Banse X, Devogelaer JP, Delloye C, Latosse A, Holmyar D, Grynpas M. Irreversible perforation in vertebral trabeculae? J Bone Miner Res 2003;18:1247–53.
[27] Mosekilde L. Normal age-related changes in bone mass, structure and strength — consequences of the remodelling process. Dan Med Bull 1993;40:65–83.
[28] Li Mosekilde. Consequences of the remodelling process for vertebral trabecular bone structure: a scanning electron microscopy study (uncoupling of unloaded structures). Bone Miner 1990;10:13–35.
[29] Keaveney TM, Yeh OC. Architecture and trabecular bone — towards an improved understanding of the biomechanical effects of age, sex and osteoporosis. J Musculoskelet Neuronal Interact 2002;3:205–8.
[30] Parfitt AM, Matthews CHE, Villanueva AR, Kleerekoper M, Frame B, Rao DS. Relationships between surface, volume and thickness of iliac trabecular bone in aging and in osteoporosis. J Clin Invest 1983;72:1396–409.
[31] Aaron JE. Bone turnover and microdamage. Adv Osteoporotic Manag 2003;2:102–10.
[32] Aaron JE. Autoclasis — a mechanism of bone resorption and an alternative explanation for osteoporosis. Calcif Tissue Res 1976;22:247–54.
[33] Fyrie DP, Hoshaw SJ, Hamid MS, Hou FJ. Shear stress distribution in the trabeculae of human vertebral bone. Ann Biomed Eng 2000;28:1194–9.
[34] Fyrie DP, Schaffler MB. Failure mechanisms in human vertebral cancellous bone. Bone 1994;15:105–9.
[35] Yeni YN, Kim D-G, et al. Human cancellous bone from T12–L1 vertebrae has unique microstructural and trabecular shear stress properties. Bone 2009;44:130–6.
[36] Melton LJ, Kan Frye MA, Wahner WH, O'Fallon WM, Riggs BL. Epidemiology of vertebral fractures in women. Am J Epidemiol 1989;129:1000–11.
[37] Hasserius R, Karlsson MK, Nilsson BE, Redlund-Johnell I, Johnell O. Prevalent vertebral deformities predict increased mortality and increased fracture rate in both men and women: a 10 year population-based study of 58 individuals from the Swedish cohort in the European Vertebral Osteoporosis Study. Osteoporos Int 2003;14:61–8.
[38] Keller TS, Hansson TH, Abram AC, Spengler DM, Panjabi MM. Regional variations in the compressive properties of lumbar vertebral trabeculae: effects of disc degeneration. Spine 1989;14:1012–9.
[39] Adams MA, Pollintine P, Tobias JH, Dolan P, et al. Intervertebral disc degeneration can predispose to anterior vertebral fractures in the thoracolumbar spine. J Bone Miner Res 2006;21:1409–16.
[40] Garner PE. Bone ageing and structural disconnection. (PhD thesis) University of Leeds; 2012.
[41] van Rietbergen B, Huiskes R, Eckstein F, Ruegsegger P. Trabecular bone tissue strains in the healthy and osteoporotic human femur. J Bone Miner Res 2003;18:1781–8.
[42] Tanck E, Bakker AD, Kregsting S, Cornelissen B, Klein-Nulend J, van Rietbergen B. Predictive value of femoral head heterogeneity for fracture risk. Bone 2009;44:590–5.
[43] Homminga J, McCreadie BR, Ciarelli TE, Weinans H, Goldstein SA, Huskies R. Cancellous bone mechanical properties from normals and patients with hip fractures differ on the structural level, not on the bone hard tissue level. Bone 2002;30:759–64.
[44] Lotz JC, Cheal EJ, Hayes WC. Stress distribution within the proximal femur during gait and falls: implications for osteoporotic fracture. Osteoporos Int 1995;5:252–61.
[45] Aaron JE. Periosteal Sharpey's fibres: a novel bone matrix regulatory system? Front Endocrinol 2012;3:1–10.
[46] Singh M, Nagrath AR, Maini MS. Changes in trabecular pattern of the upper end of the femur as an index of osteoporosis. J Bone Joint Surg 1970;52:457–67.
[47] Li B, Aspden RM. Composition and mechanical properties of cancellous bone from the femoral head of patients with osteoporosis or osteoarthritis. J Bone Miner Res 1997;12:641–51.
[48] Fabreguet I, Fechtenbaum J, Briot K, Patternotte S, Roux C. Lumbar disc degeneration in osteoporotic men: prevalence and assessment of the relation with the presence of vertebral fracture. J Rheumatol 2013;40:1183–90.
[49] Zupan J, van't Hof RJ, Vindisar F, Haring G, Trebse R. Osteoarthritic versus osteoporotic bone and intra-skeletal variations in normal bone: evaluation with μCT and bone histomorphometry. J Orthop Res 2013(July):1059–66.
[50] Linton KM, Hordon LD, Shore RC, Aaron JE. Bone mineral "quality": differing characteristics of calcified microsphere populations at the osteoporotic and osteoarthritic femoral articulation front. J Biomed Sci Eng 2014;7:739–55.
[51] Gerdhem P. Osteoporosis and fragility fractures: vertebral fractures. Best Pract Res Clin Rheumatol 2013;27:743–55.
[52] Suzuki N, Ogikubo O, Hansson T. The prognosis for pain, disability, activities of daily living and quality of life after an acute osteoporotic vertebral body fracture: its relation to fracture level, type of fracture and grade of fracture deformation. Eur Spine J 2009;18:77–88.
[53] Sverdlova N. Tensile trabeculae — myth or reality? J Musculoskelet Neuronal Interact 2011;11:1–7.
[54] Frost HM. Bone mass and the "mechanostat"; a proposal. Anat Rec 1987;219:1–9.